J. Phys. Chem. A **2003,** *107,* 5555−5560

Ab Initio Studies of Borazine and Benzene Cyclacenes and Their Fluoro-Substituted Derivatives

Kian Ping Loh,*,† S. W. Yang,†,‡ J. M. Soon,† H. Zhang,† and P. Wu‡

Department of Chemistry, National University of Singapore, 3 Science Drive 3, Singapore, and Institute of High Performance Computing, Singapore

Received: February 26, 2003; In Final Form: April 23, 2003

We have performed unrestricted density functional theory calculations for the borazine and benzene cyclacene systems to obtain insights into their structural and electronic properties as a function of the size of the cyclacene. The frontier molecular orbital gap, ΔE_{gap}, in borazine cyclacene increases steadily with the number of rings, n, and stabilizes at ~6.7 eV for $n > 9$, in contrast to the benzene cyclacene system where the gap decreases and approaches 1.13 eV for $n > 8$. For borazine cyclacene, the top and bottom trannulenes in the rings are structurally different. A stronger delocalization of π electrons in the boron-apexed trannulene compared to the nitrogen-apexed trannulene was discovered. For the carbon cyclacene, we observed alternation in both ΔE_{gap} and the bond distances as the number of electrons in the trannulene chains alternate between $4k$ and $4k + 2$. The effect of fluorine substitution on boron atoms in the borazine cyclacene increases the bonding energy and ΔE_{gap}, whereas substitution on nitrogen atoms results in the opposite. A special π-type interaction between the fluorine lone-pair p electrons and the B−N−B σ-bonding framework results in special enhancement in the stability of the F−B substituted systems. F substitution on carbon cyclacene increases the ΔE_{gap} when n is even but decreases ΔE_{gap} when n is odd.

1. Introduction

Cyclacene, a class of laterally fused benzoid hydrocarbons, offers a simple conceptual framework for understanding the structure and properties of nanotube or fullerene systems because of their remarkable similarity to these structures. A cyclacene structure consists of two types of embedded structures: an arenoid belt which is composed of benzenoid rings in the case of simple cyclacene, and annulenic peripheral rings which becomes either $4k$ or $4k + 2$ type depending on the number of benzenoid rings present. Theoretical studies on cyclacene have shown that some properties depend strongly on the length of the peripheral circuits or the number of benzenoid rings in the arenoid belt; the effect is known as "cryptoannulenic effect".[1−8]

Borazine, the inorganic analogue of benzene, is obtained by replacing the carbon atoms with alternating boron and nitrogen atoms. Extensive studies have been conducted to ascertain the aromaticity of this heterocyclic π-electron system,[9−12] but very little have been performed on the properties of the borazine cyclacene. One might consider $(BN)_n$ as possible precursors to BN nanotubes. BN cyclacene may exhibit unique host−guest chemistry when metal atoms are trapped in their cylindrical cavities. Although borazine and its derivatives have been widely studied, the aromaticity of its cyclacene counterparts is still relatively unknown. Work on borazine cyclacene is limited to that of Erkoc,[1] in which the semiempirical method, AM1-RHF, was used and the trend toward the formation of larger BN cyclacene ring is predicted to be exothermic. The major disadvantage of semiempirical and Hartree−Fock (HF) methods is their neglect of instantaneous electron correlation, and therefore, they are not accurate enough to describe the electronic properties of the systems considered. We use DFT in this study to accurately compute molecular properties because it includes electron correlation. In this work, we explore the molecular and electronic structure of the borazine cyclacene system to understand whether there is an aromatic stabilization or cryptoannulenic effect and compare it with the carbon cyclacene system. In addition, we study the fluro-substituted borazine and carbon cyclacene systems to investigate these effects with fluorine.

2. Method

Two levels of calculations have been carried out using the Gaussian 98 suite[13] on a sun supercomputer, E10K. Unrestricted density functional theory (DFT) employing Becke's three parameters hybrid method and Lee−Yang−Parr's correlation correction (UB3LYP) with a 6−31 G(d) basis set is applied in this work. The Hartree−Fock (UHF) method with a 3-21 G basis set is also used for C_n ($n = 4−9$) and $(BN)_n$ ($n = 4−12$) cyclacene to perform a pre-DFT geometrical optimization.

3. Results and Discussion

3.1. Geometry of Borazine and Benzene Cyclacenes. A drawing of the cyclacene structure for $(BN)_6$ ($n = 6$) is shown in Figure 1. Important parameters such as the distance between the apex atom and the fusion site atom (d_2, d_4), distance between the fusion site atoms (d_3), the BN_HB angle β, the NB_HN angle α, and the dihedral angles γ and δ are indicated. Changes in structural parameters with the ring size n can be used to study the relationship between structure, strain, and electron delocalization in the peripheral circuits. A short d_3, for example, will indicate effective coupling between the two trannulene rings, whereas a shorter d_2 and longer d_3 will indicate stronger intrachain bonding within one trannulene ring. Changes in the

---

* To whom correspondence should be addressed. E-mail: chmlohkp@nus.edu.sg.

[†] National University of Singapore.

[‡] Institute of High Performance Computing.

10.1021/jp030254h CCC: \$25.00

TABLE 1: Structure Parameters of $(BN)_n$ Cyclacenes as a Function of Ring Size (n) after Full Geometrical Optimization

n	group point	dip. m. (debye)	d_1 (Å)	d_2 (Å)	dip. m. D (d_2)	d_3 (Å)	dip. m. D (d_3)	d_4 (Å)	dip. m. D (d_4)	d_5 (Å)	α ∠NBN	β ∠BNB	γ B-top	δ N-top	d_B^P	d_N^P
4	C_{4v}	4.53	1.108	1.472	5.16	1.457	6.63	1.473	8.12	1.192	115.1	99.8	25.4	51.3	0.158	0.452
5	C_{5v}	6.02	1.016	1.459	4.98	1.457	6.43	1.46	7.84	1.192	116.5	106.4	19.7	44.2	0.115	0.358
6	C_{6v}	7.42	1.015	1.452	4.92	1.457	6.32	1.454	7.68	1.192	117.3	110.6	16.8	38.5	0.098	0.296
7	C_{7v}	8.80	1.015	1.448	4.88	1.457	6.24	1.451	7.59	1.192	117.9	115.1	14.7	34.2	0.081	0.248
8	C_{8v}	10.20	1.015	1.446	4.87	1.457	6.21	1.449	7.56	1.193	118.3	115.1	13.4	30.6	0.071	0.217
9	C_{9v}	11.60	1.014	1.444	4.87	1.457	6.20	1.448	7.55	1.192	118.7	116.6	12.1	27.5	0.103	0.190
10	C_{10v}	13.05	1.014	1.442	4.87	1.457	6.20	1.447	7.54	1.193	118.9	117.7	11.4	25.2	0.096	0.167
11	C_{11v}	14.39	1.014	1.441	4.89	1.458	6.21	1.446	7.55	1.193	119.2	118.4	10.5	23.2	0.040	0.152
12	C_{12v}	15.79	1.014	1.440	4.90	1.458	6.22	1.446	7.55	1.193	119.4	119.1	9.7	21.4	0.023	0.138

bond angles toward 120° will indicate a greater degree of aromatization. The structural parameters for $(BN)_n$ cyclacenes after optimizing the geometry are listed in Table 1. Our DFT calculations show that $(BN)_n$ has a C_{nv} point group.

3.2. Borazine Cyclacene. The bond lengths between the fusion atom and peripheral atom, r_{N-BH} (d_2) and r_{B-NH} (d_4), decrease from 1.472 to 1.440 Å, and 1.473 to 1.446 Å, respectively, when n increases. In addition, as n increases, these atoms become more sp^2-like with a flattening of the rings and bond angles approaching 120°. The distance between fusion site atoms, r_{B-N}, (d_3), is relatively constant at 1.457 Å (± 0.001 Å).

In the single borazine molecule, the bond angle α (∠NBN, 117.2°) is smaller than β (∠BNB 122.8°). One way to understand this is based on the tight binding concept where the smaller nitrogen atom in BNB can sit deeper between the B atoms, resulting in a shorter BN bond length, and consequently a larger BNB angle compared to the NBN angle. However, in borazine cyclacene, the trend is reversed, i.e., $\angle\alpha > \angle\beta$. Both ∠α and ∠$\beta$ approach the idealized sp^2 bond angle of 120° with an increase in the ring size. Because of the empty p orbital on boron, it is easier for the boron atom to adopt a 120° trigonal planar configuration compared to the nitrogen atom. To quantify this effect, we calculated the projected distance of the fusion atom B to the planes of the three nitrogen atoms bonded to it, which we denote as d_B^P. Likewise, the projected distance of fusion atom N to the three boron atoms bonded to it is denoted as d_N^P. It is significant that $d_B^P < d_N^P$, suggesting that the drive toward "trigonal co-planarization" is much stronger in the fusion site boron atom compared to the fusion nitrogen atoms. For example, for $(BN)_6$, $d_B^P = 0.098$ Å, whereas $d_N^P = 0.296$ Å. To achieve a small d_B^P value when the ring size is small, the atoms in the peripheral circuit have to tilt toward the fusion atoms to achieve coplanarization with the latter. For example, the apex N, in the triangle labeled $B'N_HB'$, must tilt away from its $B'B'N'N'$ plane and move toward the fusion boron (in the process increasing dihedral angles). The results indicate that the dihedral angle is higher when N is the apex atom and B is the fusion atom compared to the case when they are switched, especially in the borazine cyclacene systems with smaller ring size. This contributes to an asymmetry in the borazine cyclacene structure due to the greater outward bending of the N-apex atoms from the $B'B'NN$ plane compared to the side with B as the apex atoms; Figure 1 illustrates this. In this respect, the borazine cyclacene shares some similarity with BN nanotubes. Menon et al. did a generalized tight-binding molecular dynamics (GTBMD) relaxation on a (10,0) BN nanotubes and observed that the B atoms rotate inward to an approximate planar configuration, whereas the N atoms move outward into a corresponding pyramidal configuration.[14]

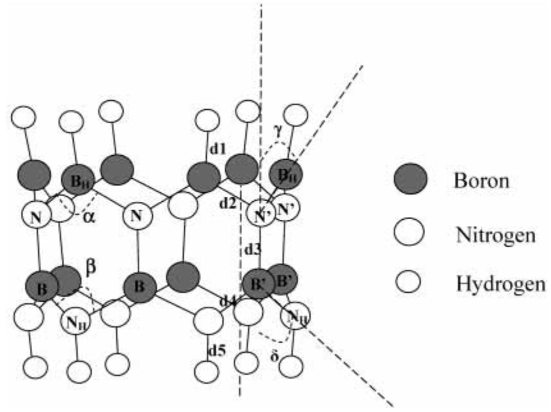

Figure 1. Schematic drawing of the $(BN)_6$ cyclacene structure: d_2 and d_4 are the distances between the apex atom and fusion site atom, and d_3 is the distance between two fusion site atoms. α is the NB_HN angle, and β is the BN_HB angle. γ is the dihedral angle between plane $N'B_HN'$ and fusion atom plane $B'B'N'N'$, and δ is is the dihedral angle between plane $B'N_HB'$ and fusion atom plane $B'B'N'N'$.

Another way to explain the larger NBN angle compared to the BNB angle is by studying how these angles change with ring size, as indicated in Table 1. It can be seen that ∠α is closer to 120° compared to ∠β for all values of n. This suggests that the top trannulene where B forms the apex atoms has a greater degree of electron delocalization within the peripheral circuit than the bottom trannulenic ring where N forms the apex atoms. The back-transfer of π electrons from N to B reduces the charge density on B and N. The dipole moment, D, calculated according to the following formula $D = r\delta_{\text{charge}}$,[15] is smaller on the B-apex annulenic ring than the N-apex annulenic ring. This increase in bond order should result in a shortening of the distance between B and N. Indeed, our results in Table 1 show that the bond length d_2 is smaller than d_4. Clearly, π-electron delocalization is more effective along the top trannulenic chain when the B atom is the apex.

3.3. Carbon Cyclacene. According to our DFT calculations, the symmetry of carbon cyclacene is D_{nh}. Table 2 shows the structural parameters of the carbon cyclacenes with various ring sizes. The bond distance between the fusion and peripheral atoms (d_2 and d_4) decreases from 1.447 to 1.411 Å as n increases from 4 to 9. The bond lengths between two fusion atoms (d_3) in the carbon cyclacene exhibit significant bond length alternation (0.03−0.06 Å) as n varies; this is shown in the plot in Figure 2. The alternation in d_3 suggests that the coupling between the two peripheral trannulene chains is alternatively strong and weak as n varies; no doubt a consequence of the alternation between $4k$ and $4k + 2$ π electrons. Such a change is not observed in the $(BN)_n$ system where d_3 remains effectively constant.

In the carbon cyclacene system, the bond angles α and β (Table 2) are effectively similar because the trannulenes on the two sides are similar. When comparing structures with similar ring size, the α angles of the carbon cyclacene are not as close

TABLE 2: Structural Parameters of Carbon Cyclacene as a Function of Ring Size (*n*) after Full Geometrical Optimization

n	group point	dip. m. (debye)	d_1 (Å)	d_2 (Å)	d_3 (Å)	d_4 (Å)	d_5 (Å)	α ∠CC_HC	β <∠CC_HC	γ C	δ C	d_C^P	$d_C^{P'}$
4	D_{4h}	0.00	1.086	1.447	1.411	$=d_2$	$=d_1$	112.9	=α	28.8	$=\gamma$	0.376	$=d_C^P$
5	D_{5h}	0.00	1.088	1.422	1.474	$=d_2$	$=d_1$	112.8	=α	30.4	$=\gamma$	0.249	$=d_C^P$
6	D_{6h}	0.00	1.088	1.418	1.451	$=d_2$	$=d_1$	115.4	=α	26.9	$=\gamma$	0.206	$=d_C^P$
7	D_{7h}	0.00	1.088	1.413	1.471	$=d_2$	$=d_1$	117.2	=α	22.6	$=\gamma$	0.178	$=d_C^P$
8	D_{8h}	0.00	1.088	1.411	1.459	$=d_2$	$=d_1$	118.3	=α	20.8	$=\gamma$	0.149	$=d_C^P$
9	D_{9h}	0.00	1.088	1.410	1.470	$=d_2$	$=d_1$	119.0	=α	18.0	$=\gamma$	0.140	$=d_C^P$

TABLE 3: Values of ΔE_{gap}, HOMO and HOMO − 1, $\Delta_{(-1)-(0)}$, and LUMO and LUMO + 1 for Borazine Cyclacene as a Function of *n* (Unit: eV)

n	bonding energy	HOMO (−1)	$\Delta_{(-1)-(0)}$	HOMO	Δ_{gap}	LUMO	$\Delta_{(+1)-(0)}$	LUMO (+1)
4	−138.70	−6.70	0.01	−6.70	3.78	−2.92	2.55	−0.37
5	−177.27	−6.62	0.00	−6.62	4.68	−1.94	1.73	−0.21
6	−215.22	−6.91	0.11	−6.80	5.58	−1.21	1.11	−0.10
7	−252.81	−6.63	0.00	−6.63	5.96	−0.67	0.73	0.06
8	−290.19	−6.77	0.00	−6.77	6.52	−0.25	0.48	0.23
9	−327.44	−6.65	0.00	−6.65	6.72	0.07	0.15	0.23
10	−364.60	−6.66	0.00	−6.66	6.87	0.21	0.01	0.21
11	−401.68	−6.66	0.00	−6.66	6.79	0.12	0.00	0.12
12	−438.71	−6.63	0.00	−6.63	6.74	0.11	0.00	0.11

to 120° as the trannulene with the B-apexed side. This reinforces the concept that the driving force for trigonal planarisation on boron is strong. The dihedral angles of the carbon cyclacenes are larger than that of the B-apexed trannulene in borazine cyclacene but smaller than that of N-apexed trannulene, i.e., d_C^P is larger than d_B^P but smaller than d_N^P.

3.4. Energy and Molecular Orbital of Carbon Cyclacene. Table 3 presents the energies and frontier molecular orbital (MO) information for the borazine cyclacenes. Our DFT calculations show that the binding energies of $(BN)_n$ increase with ring size, suggesting that the formation of bigger ring structures is exothermic. Figure 3 shows the plot of frontier HOMO−LUMO separation, ΔE_{gap}, for carbon and borazine cyclacenes versus the number of rings, *n*, where interesting differences between the C_n and $(BN)_n$ structures can be seen. The results indicate that ΔE_{gap} of $(BN)_n$ *increases* monotonically with *n* until $n = 10$, where it stabilizes at 6.7 eV.

In the previous section, we have shown that the bond length between the two fusion carbon atoms (d_3) exhibits alternation when *n* changes between odd and even. A similar trend is also observed for ΔE_{gap}. We used the frontier molecular orbitals for the C_n systems (Table 4) in an attempt to understand how changes in the number of electrons in the peripheral circuit affect the energy of the frontier orbitals. It is very interesting that the energy gaps between HOMO and HOMO − 1 ($\Delta_{(-1)-(0)}$) as well as LUMO and LUMO + 1($\Delta_{(0)-(+1)}$) alternate between zero and nonzero values. The same fluctuation can be found in $\Delta_{(-2)-(-1)}$. These MO levels can be presented graphically in Figure 4. When *n* is odd, the electron number is $4k + 2$ and $\Delta_{(-1)-(0)} = 0$; that is, the orbitals are degenerate. In this case, ΔE_{gap} is higher than the case when *n* is even. The frontier MOs for $n = 7$ are graphically presented in Figure 5. The HOMO and HOMO − 1 are degenerate, as well as the LUMO and LUMO + 1. The HOMO and HOMO − 1 are clearly π-like in character with the orbitals spreading between the peripheral and fusion-site carbon atoms, which is evident of the aromatic character of the $4k + 2$ system. The side view clearly shows that there is no coupling between the HOMO orbitals of the two trannulene chains.

Two types of interactions are operative in the carbon cyclacene systems here, namely, intrachain interactions within individual trannulene and interchain interactions between the two trannulenes. For the case where *n* is odd, the intrachain interaction within individual trannulene is of the (4k + 2) type; hence, each trannulene is aromatic and stable. The large ΔE_{gap} can be explained using the simple MO diagram presented in Figure 4a. When the π-electron count in each peripheral

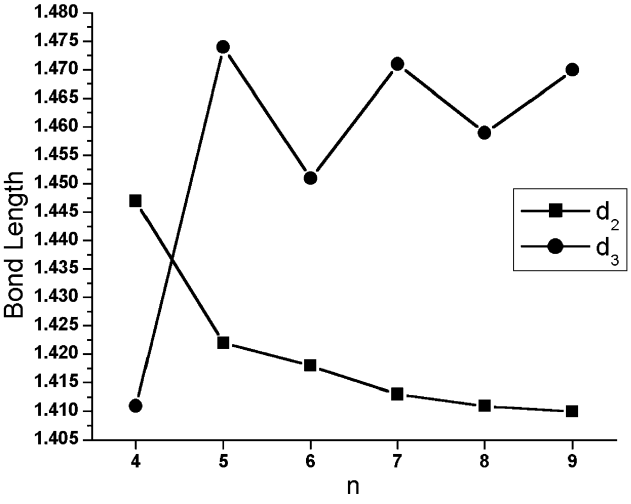

Figure 2. Variation of d_2 and d_3 in carbon cyclacene as a function of *n*. Bond lengths are in angstroms.

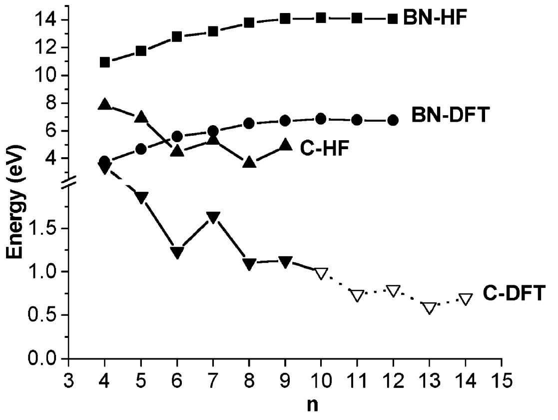

Figure 3. Frontier molecular orbital energy gap for HF (UHF/3-21G) and DFT (UB3LYP/6-31G(d)), respectively.

TABLE 4: Value of Δ_{gap}, HOMO and HOMO − 1, $\Delta_{(-1)-(0)}$, and LUMO and LUMO + 1 for Carbon Cyclacene as a Function of n[a]

n	bonding energy	HOMO (−1)	$\Delta_{(-1)-(0)}$	HOMO	Δ_{gap}	LUMO	$\Delta_{(+1)-(0)}$	LUMO (+1)
4	−154.7	−5.70	0.80	−4.90	3.43	−1.47	0.16	−1.31
5	−196.6	−4.32	0.00	−4.32	1.87	−2.45	0.63	−1.82
6	−240.3	−5.50	1.69	−3.81	1.24	−2.57	0.86	−1.71
7	−283.0	−4.06	0.00	−4.06	1.65	−2.41	0.00	−2.41
8	−326.2	−4.96	1.07	−3.89	1.11	−2.79	1.08	−1.71
9	−367.9	−3.92	0.00	−3.92	1.13	−2.79	0.00	−2.79

[a] Note that the energy gaps between HOMO and HOMO − 1, $\Delta_{(-1)-(0)}$, as well as LUMO and LUMO + 1, alternate between zero and nonzero values. (Units: eV.)

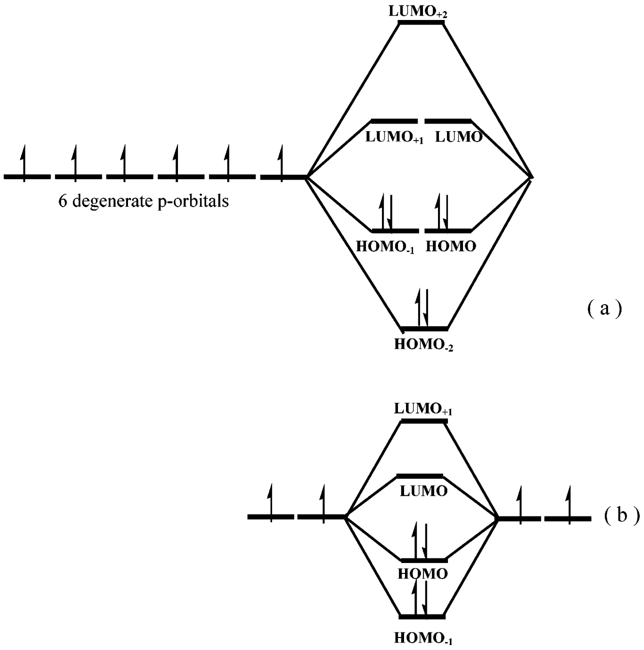

Figure 4. Structure of frontier molecular orbitals of (a) $(4k + 2)$ carbon cyclacene, where $n = 6$, HOMO and HOMO − 1 are degenerate; (b) $(4k)$ carbon cyclacene, where $n = 7$. HOMO and HOMO − 1 are nondegenerate.

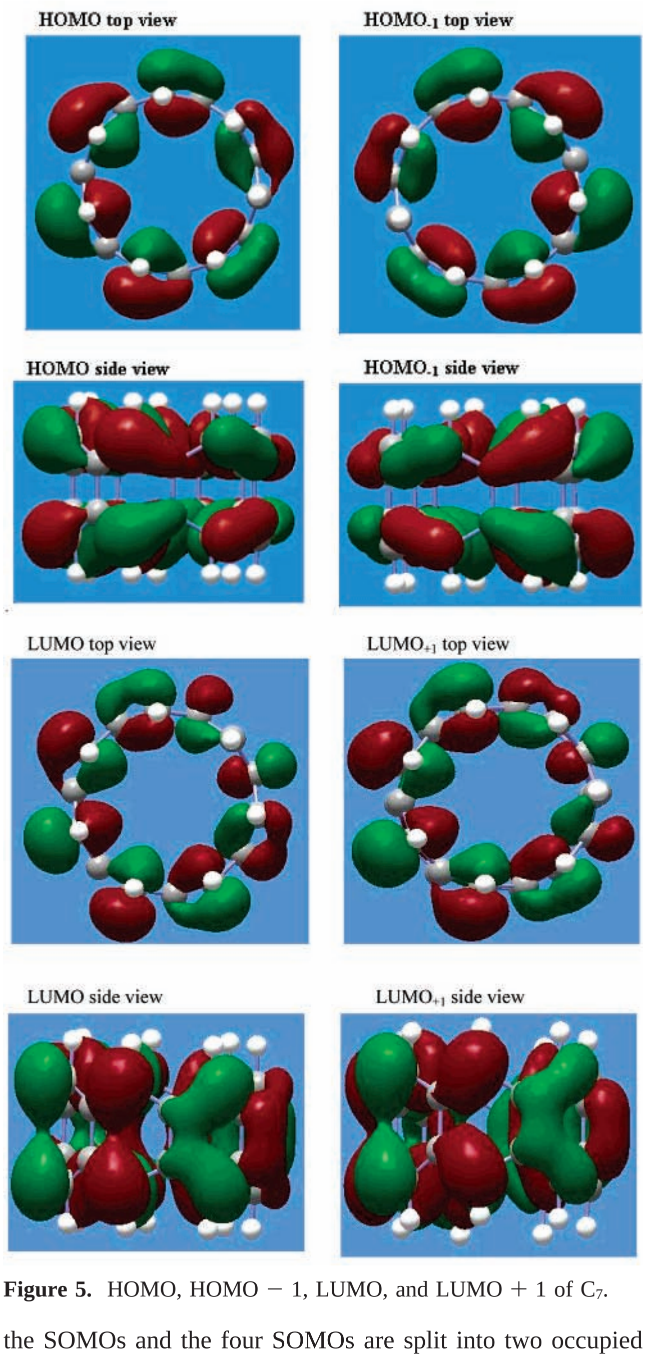

Figure 5. HOMO, HOMO − 1, LUMO, and LUMO + 1 of C_7.

trannulene is of the 4k + 2 type, the bonding MOs are all doubly occupied, leaving the antibonding MOs empty. Consequently, first-order Peierls stabilization of the bonding MOs and simultaneous destabilization of the antibonding MOs will result in a large ΔE_{gap}.

When n is even, the electron number is $4k$. The frontier MOs presented for the $n = 6$ case in Figure 6 shows that HOMO and HOMO − 1 are not degenerate and distinct differences in the shape of the MOs can be seen. The HOMO and LUMO consist of six isolated orbitals centered on the peripheral (or apex) carbon atoms. In our previous discussion, we pointed out that the r_{C-C} bond length (d_3) is longer when n is odd $(4k + 2)$ compared to when n is even $(4k)$. This idea is fully expressed in the MO diagrams in Figures 5 and 6 where the shape of the HOMO for $n = 7$ $(4k + 2)$ shows intrachain interaction (top-view) and the absence of interchain interaction (side view), whereas that for $n = 6$ $(4k)$ shows the absence of intrachain interaction and presence of coupling between the interchain MOs.

The $4k$-electron count in the peripheral trannulene means that the two antibonding MOs are singly occupied. Triplet states are favored in these two singly occupied molecular orbitals (SOMOs), as the singlet states are anti-aromatic and unstable.[14] In such a situation where the triplet state is favored, first-order Peierls effect is not possible. To attain stabilization, the two $[4k]$ trannulene moieties in a carbon cyclacene couple through the SOMOs and the four SOMOs are split into two occupied bonding MO (HOMO and HOMO − 1) and two unoccupied antibonding MOs (LUMO and LUMO + 1), as illustrated in Figure 4b. The consequence is a smaller ΔE_{gap}. This coupling also results in shorter r_{C-C} bonds (d_3) when n is even (Table 2).

3.5. Energy and Molecular Orbital of Borazine Cyclacene. Even though $(BN)_n$ cyclacenes are isoelectronic with C_n

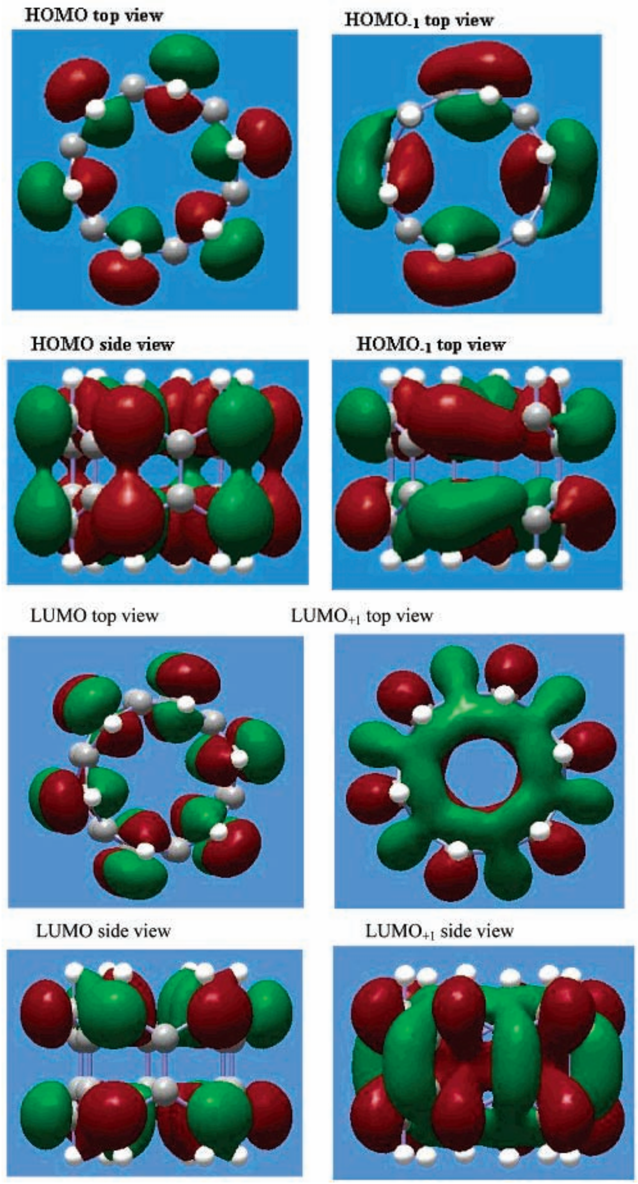

Figure 6. HOMO, HOMO − 1, LUMO, and LUMO + 1 of C_6.

cyclacenes, their electronic properties are vastly different. The $(BN)_n$ frontier MO energy levels in Table 3 show that $\Delta_{(-1)-(0)} = 0$ for almost all systems. This implies that the HOMO and HOMO − 1 orbitals are degenerate and that there is no additional coupling between the two trannulenic rings that arise from "SOMO" type p orbitals. For example, there are no delocalized π orbitals in the HOMO and HOMO − 1 for $(BN)_6$. In this case, the HOMO consists of a series of small orbitals isolated on a single atom and are *more σ-like*, resulting in an energy lowered by about 2.3∼3.0 eV compared to that of the C_n system. The poor aromaticity throughout the series of n for $(BN)_n$ means that ΔE_{gap} is not affected by an alternation of the peripheral electrons between $4k$ and $4k + 2$ (assuming electrons from N lone pairs). The absence of coupling precludes the effect of splitting the frontier MOs and narrowing the gap. In fact, ΔE_{gap} increases when n increases for the $(BN)_n$ systems. A tiny fluctuation can be detected in the energies of the HOMO (Table 3) when n is odd and even for $n \leq 6$. This can be explained by the larger overlap of p orbitals in small-rings systems.

3.6. Structure, Energy, and Molecular Orbital of F-Substituted Carbon Cyclacene. There is an interesting variation in the band gap of the carbon cyclacene with ring size when one side of the carbon cyclacene is substituted with fluorine. Figure 7 plots the changes in ΔE_{gap} with n for carbon cyclacene with and without F substitution. Intriguingly, when n is odd, ΔE_{gap} decreases compared to the unsubstituted structure, whereas when n is even, ΔE_{gap} increases. The geometry of the fluoro-substituted cyclacene shows no change in the distance between the two fusion site carbons (d_3), although the distance between the fusion and peripheral C atoms (d_2 and d_4) shortens after F substitution, resulting in a contraction in the size of the F-substituted peripheral annulenic ring. A conjugation effect is apparent because both d_4 and d_2 have reduced relative to d_3, suggesting that π electrons contribute in the direction of the fluoro-substituted site. For carbon cyclacene with an odd number of rings, the addition of F disturbs the $4k + 2$ electron network by reducing the electron density in the peripheral network and making it slightly less aromatic. This effect is apparent whether the F substitution occurs on one side or on two sides. When n is even, the effect is the opposite. The electronegative F reduces the electron density in the $4k$-electron network and improves the aromaticity of the system.

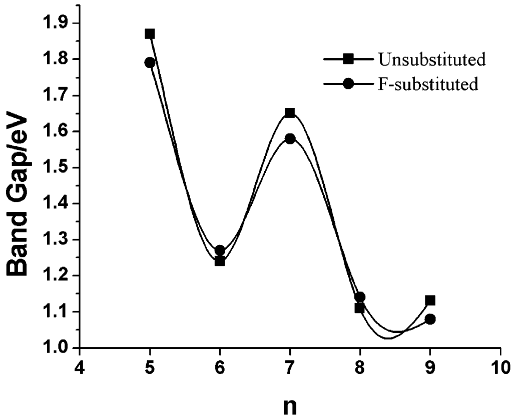

Figure 7. Variation in ΔE_g for unsubstituted cyclacene and after F substitution along one peripheral ring. ΔE_g is lowered when n is odd and increased when n is even.

Frequency analysis is one way of analyzing the degree of aromaticity along the peripheral chain. An increase in the frequency of the C−C stretch is evidence of an increase in bond order due to π-electron delocalization. The IR shifts as well as their intensities are listed in Table 5. The radial breathing mode of the ring in an "in−out" fashion perpendicular to the principal axis of the cyclacene dominates at first for the unsubstituted carbon cyclacene, as can be judged from the stronger intensities of these vibrations. However, with the substitution of the F on one side of the ring, the "up−down" vibration parallel to the principal axis of the cyclacene mode now predominates.

As seen in Table 5, the stretching vibration mode of the C−C in the peripheral chain for the unsubstituted carbon cyclacene experiences an alternation that is in line with the changes in the aromaticity. When n is odd and the electron count in the chain is $4k + 2$ and aromatic, the stretching frequency is higher than when n is even ($4k$ and unaromatic). Interestingly, substitution of fluorine on one side of the chain results in a reversal of this trend, although there is no change in the d_3 distance. The C−F stretching frequency, as well as the C−C stretch in the peripheral chain that is coupled to it, is higher when n is even compared to when n is odd. The fluorine p electrons can be delocalized into the π-bonding network of the chain. The higher frequencies observed for the C−F stretch and the C−C stretch in the peripheral chain for the carbon cyclacene with even n indicates that the in-plane overlap of the $4k$ π electrons with the p electrons from fluorine is more favorable

TABLE 5: IR Vibrational Peaks Calculated for Carbon Cyclacene Systems and Their Fluorinated Counterparts

n	unsubstituted carbon cyclacene C−C stretch in peripheral ring (cm^{-1})	unsubstituted carbon cyclacene radial breathing mode (cm^{-1})	fluorinated carbon cyclacene C−C stretch in peripheral ring (cm^{-1})	C−F vibrational mode (cm^{-1})
5	1245.5 (0.01)	661.6 (1.00)	1449.7 (1.00)	1054.3 (0.16)
6	1241.6 (0.15)	678.0 (0.59)	1495.7 (0.59)	1067.5 (0.10)
7	1266.5 (0.08)	717.5 (0.74)	1476.8 (1.00)	1065.6 (0.16)
8	1260.6 (0.18)	722.8 (0.20)	1501.7 (0.73)	1072.9 (0.13)
9	1271.8 (0.15)	740.1 (0.13)	1488.8 (1.00)	1070.3 (0.15)

compared to the $4k + 2$ π electron systems. This suggests that F substitution enhances the aromaticity of the $4k$ system but decreases the aromaticity of the $4k + 2$ system.

3.7. Structure, Energy, and Molecular Orbital of F-Substituted Borazine Cyclacene. The IR vibrational data indicate that the breathing frequency for the borazine cyclacene increases as *n* is increased; this follows the trend in the decrease of the peripheral B−N bond length with ring size. Notably, the average vibration frequency for the borazine cyclacene is higher than their carbon cyclacene counterparts because of the increased bond strength of the B−N system.

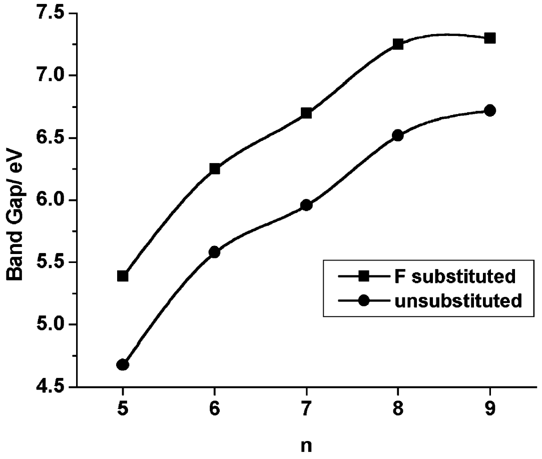

Figure 8. Change in ΔE_g for borazine cyclacene before and after F substitution on the B-peripheral side.

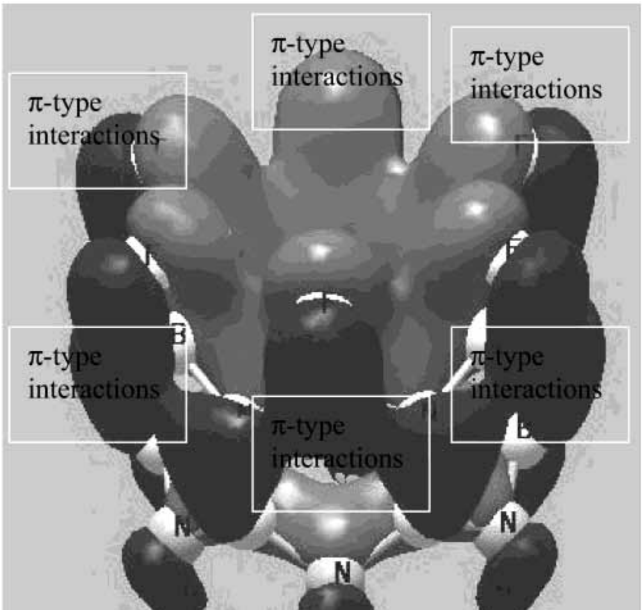

Figure 9. In-plane overlap between the F 2p orbital with the B−N−B σ-bonding framework of the hexa-fluoro substituted borazine cyclacene. The six π-type interactions are labeled in the diagram.

When the F is substituted on the B peripheral side, the breathing vibration mode experiences a general increase compared to the unsubstituted borazine cyclacene. The position of the F substitution affects the bonding energy and ΔE_{gap} of the system; when F is attached to B, it increases, and it decreases when F is attached to N. The increase in ΔE_{gap} is observed for all *n* when the F substitution is on the boron site, as shown by the plot in Figure 8. For fluorine substitution on B, a special π-type interaction between the p electrons of the fluorine lone pair and the B−N−B σ-bonding framework results in special enhancement of the stability of the F−B substituted systems. Figure 9 shows the MO for $n = 6$ hexa-substituted borazine where the hydrogen atoms on one peripheral side have been replaced by F atoms. The spread of the in-plane π-type orbitals can be seen for all 6 F atoms. In contrast, full F substitutions on the top N atoms will result in the smallest bonding energy as well as smallest ΔE_{gap}.

4. Conclusion

We have performed ab intio studies on the carbon cyclacene and borazine cyclacene systems and analyzed the differences in aromaticity between these two systems. A fluctuation in the structural parameters, as well as the frontier orbital energy separation, ΔE_{gap}, as a function of the ring size, is observed in the carbon cyclacene system. This is not observed in the borazine cyclacene system, although it was found that the delocalization of electrons along the boron-apex ring is more efficient than that of the nitrogen-apex ring. The ΔE_{gap} of the borazine cyclacene system increases with the ring size, in contrast to the carbon cyclacene system.

The effects of fluorination along one peripheral ring of the C and BN cyclacene were also studied. It was found that F substitution along the B-apexed side of borazine cyclacene resulted in an increase in the frontier orbital gap, whereas similar substitution along the N-apexed side resulted in a decrease of the gap. In contrast, F-substitution along the peripheral chain of the carbon cyclacene increased the frontier orbital band gap when *n* is even and decreased it when *n* is odd.

References and Notes

(1) Erkoc, S. *J. Mol. Struct. (THEOCHEM)* **2001**, *540*, 153.
(2) Parker, J. K.; Davis, S. R. *J. Phys. Chem.* **1997**, *101*, 9410.
(3) Turker, L. *Polycyclic Aromat. Compd*. **1997**, *12*, 213.
(4) Turker, L. *J. Mol. Struct. (THEOCHEM)* **1998**, *454*, 83.
(5) Erkoc, S. *J. Mol. Struct. (THEOCHEM)* **2002**, *578*, 65.
(6) Turker, L.; Erkoc, S. *J. Mol. Struct. (THEOCHEM)* **2001**, *531*, 401.
(7) Erkoc, S. *J. Mol. Struct. (THEOCHEM)* **2001**, *542*, 84.
(8) Turker, L. *J. Mol. Struct. (THEOCHEM)* **2000**, *531*, 175.
(9) Chiavarino, B.; et al. *J. Am. Chem. Soc.* **1999**, *121*, 11204.
(10) Beachley, O. T., Jr. *J. Am. Chem. Soc.* **1970**, *92*, 5372.
(11) Fower, P. W.; Steiner, E. J. *J. Phys. Chem. A* **1997**, *101*, 1409.
(12) Dennis, G. R.; Ritchie, G. L. D. *J. Phys. Chem.* **1993**, *97*, 8403.
(13) Foresman, J. B.; Frisch, E. *Exploring Chemistry with Electronic Structure Methods*; Gaussian: Pittsburgh, PA, 1996.
(14) Menon, M.; Srivastava, D. *Chem. Phys Lett.* **2000**, *307*, 407.
(15) Choi, H. S.; Kim, K. S. *Angew. Chem., Int. Ed.* **1999**, *38*, 2256.